Generation of a monkey-tropic human immunodeficiency virus type 1 carrying *env* from a CCR5-tropic subtype C clinical isolate

Hiroyuki Otsuki, Mai Yoneda, Tatsuhiko Igarashi, Tomoyuki Miura*

Laboratory of Primate Model, Experimental Research Center for Infectious Diseases, Institute for Virus Research, Kyoto University, 53 Shogoin Kawara-cho, Sakyo-ku, Kyoto, 606-8507, Japan.

* Corresponding author: Institute for Virus Research, Kyoto University, 53 Shogoin Kawara-cho, Sakyo-ku, Kyoto, 606-8507, Japan.
Phone: 81-75-751-3984, Fax: 81 75 761 9335.
E-mail addresses: tmiura@virus.kyoto-u.ac.jp

Abstract, 149 words; Main text, 6202 words; Figure legends, 568 words

Abstract

Several derivatives of human immunodeficiency virus type 1 (HIV-1) that evade macaque restriction factors and establish infection in pig-tailed macaques (PtMs) have been described. These monkey-tropic HIV-1s utilize CXCR4 as a co-receptor that differs from CCR5 used by most currently circulating HIV-1 strains. We generated a new monkey-tropic HIV-1 carrying *env* from a CCR5-tropic subtype C HIV-1 clinical isolate. Using intracellular homologous recombination, we generated an uncloned chimeric virus consisting of at least seven types of recombination breakpoints in the region between *vpr* and *env*. The virus increased its replication capacity while maintaining CCR5 tropism after *in vitro* passage in PtM primary lymphocytes. PtM infection with the adapted virus exhibited high peak viremia levels in plasma while the virus was undetectable at 12 - 16 weeks. This virus serves as starting point for generating a pathogenic monkey-tropic HIV-1 with CCR5-tropic subtype C *env*, perhaps through serial passage in macaques.

Keywords:
Monkey-tropic HIV-1
Pig-tailed macaque

Intracellular homologous recombination

Primary isolate

Subtype C

CCR5 tropism

In vitro passage

Animal model

AIDS

Restriction factor

41 **Introduction**

42 Nonhuman primate models with human-like immune systems are often employed to
43 evaluate the efficacy of candidate vaccines against acquired immune deficiency
44 syndrome (AIDS). However, human immunodeficiency virus type 1 (HIV-1) infects
45 humans or chimpanzees (*Pan troglodytes*) but not rhesus macaques (*Macaca mulatta*),
46 the most widely used primate species in biomedical research (Gibbs et al., 2007).
47 Experimental infection of macaques with simian immunodeficiency virus (SIV) or
48 simian-human immunodeficiency virus (SHIV) has been used extensively to investigate
49 HIV-1 infection *in vivo*. Pathogenic infection with SIV allows insight into the
50 mechanisms of pathogenesis and provides information for development of novel
51 vaccination strategies. However, due to the marked antigenic difference in viral proteins
52 between HIV-1 and SIV, macaque models with SIV are not suitable for evaluating the
53 immune response directed against HIV-1 (Javaherian et al., 1992; Kanki et al., 1985;
54 Murphey-Corb et al., 1986). SHIV, a chimeric virus carrying *tat, rev, vpu* and *env* from
55 HIV-1 with an SIV genetic backbone, has been constructed and used widely to assess
56 the immune response and pathogenicity directed against HIV-1 Env (Shibata and

57 Adachi, 1992; Reimann, et al., 1996; Harouse, et al., 1999)

58 Highly pathogenic SHIV irreversibly depletes circulating $CD4^+$ T-lymphocytes,
59 and cause rapidly AIDS-like symptoms in infected macaques. These properties are,
60 however, different from the vast majority of circulating HIV-1 or SIV isolates, and the
61 discrepancy would be attributed to the viral co-receptor preference (Nishimura et al.,
62 2004). Entry of HIV-1 into cells is mediated through the interaction of viral envelope
63 protein with cellular CD4 and subsequent binding to either the CCR5 or CXCR4
64 chemokine receptor or both receptors. The vast majority of HIV-1 clinical isolates
65 preferentially utilize CCR5 as the co-receptor for entry (Choe et al., 1996). The
66 CXCR4-tropic or dual-tropic viruses that utilize both CCR5 and CXCR4 emerge during
67 late stages in the disease course (Doranz et al., 1996; Feng et al., 1996).

68 In addition to the co-receptor usage, it is necessary to consider the variation of env
69 gene in SHIV construction. Most HIV-1 strains currently circulating belong to group M,
70 consisting of subtypes A–D, F–H, J, K and their recombinants, and are largely
71 responsible for the global AIDS pandemic (Hemelaar, 2012). Most of early SHIVs are
72 generated by utilizing genes derived from subtype B viruses, which comprise an

73 estimated 11% of the global prevalence of HIV-1. By contrast, subtype C is the
74 dominant subtype, accounting for almost 50% of global infections. Subtype C viruses
75 do not share the antigenicity of Env as the main target of neutralizing antibodies with
76 subtype B viruses (Choisy et al., 2004; Gaschen et al., 2002). The V3 loop region of the
77 subtype C envelope is less variable than that of other subtypes (Kuiken et al., 1999), and
78 mutations appear to accumulate in the C3 and V4 regions, which are targets of
79 autologous neutralizing antibody responses in individuals infected with subtype C
80 viruses (Moore et al., 2008; Moore et al., 2009). The structure of these epitopes is
81 dissimilar between subtypes B and C (Gnanakaran et al., 2007). There are pathogenic
82 SHIVs that encode CCR5 tropic subtype C env gene (Ndung'u et al., 2001; Ren et al.,
83 2013; Song et al., 2006).

84 Conventional SHIV that encodes SIV sequence in 5' half of the genome has
85 limited utility in the evaluation of cell-mediated immunity induced by a vaccine because
86 it does not contain HIV-1 Gag in its genome; consequently, SHIV has different major
87 epitopes for cytotoxic T lymphocytes (CTLs) known to be associated with lowering the
88 plasma viral load in HIV-1 infection (Goulder and Watkins, 2004; Kiepiela et al., 2007).

89 Recently, two major restriction factors were reported to block HIV-1 replication in
90 monkey cells in a species-specific manner (Neil and Bieniasz, 2009). The restriction
91 factor apolipoprotein B mRNA-editing enzyme-catalytic polypeptide-like 3G
92 (APOBEC3G) protein is incorporated into viral particles and induces hypermutation in
93 proviral DNA in target cells mediated by its cytidine deaminase activity (Sheehy et al.,
94 2002). Macaque APOBEC3G proteins are counteracted by the SIV Vif protein but not
95 by HIV-1 Vif (Mariani et al., 2003). The other major restriction factor that inhibits the
96 viral replication cycle is tripartite motif 5α (TRIM5α) protein, which directly recognizes
97 incoming viral capsid (CA) (Stremlau et al., 2004). HIV-1 CA can bind cyclophilin A
98 (CypA), a ubiquitous cytosolic protein, to evade restriction by human TRIM5α, whereas
99 the CypA-binding activity appears to enhance TRIM5α recognition in macaque cells
100 (Berthoux et al., 2005; Keckesova et al., 2006; Stremlau et al., 2006). It is known that
101 the host species barrier of Pig-tailed macaques (PtMs) (*Macaca nemestrina*) against
102 HIV-1 is weaker than other macaques because they do not have the TRIM restriction
103 (Brennan et al., 2008).

104 Based on these findings, derivatives of HIV-1 that has a remarkably different

105 structure from the conventional SHIV were constructed by the introduction of minor
106 genetic modifications into its genome to overcome the restriction factors in macaque
107 cells. Hatziioannou et al. (2006) generated simian-tropic HIV-1 (stHIV-1) by replacing
108 the entire *vif* gene of HIV-1 with that of SIVmac or HIV type 2. Kamada et al. (2006)
109 reported the monkey-tropic HIV-1 (HIV-1mt) NL-DT5R, in which the CypA-binding
110 motif of the CA protein is substituted by the corresponding sequence of SIVmac, and
111 the entire *vif* gene is also substituted. Thippeshappa et al. (2011) generated HSIV-vif, a
112 clone of HIV-1 by substituting the *vif* gene with that of a pathogenic SIVmne clone.
113 These derivatives of HIV-1 established persistent infection in PtMs for months but were
114 controlled thereafter (Hatziioannou et al., 2009; Igarashi et al., 2007; Thippeshappa et
115 al., 2011). These monkey-tropic HIV-1 derivatives currently available are not
116 CCR5-tropic; NL-DT5R and HSIV-Vif encode *env* from a CXCR4-tropic, and stHIV-1
117 encodes *env* from dual-tropic subtype B viruses.

118 In this study, we generated a new HIV-1mt strain carrying *env* from a CCR5-tropic
119 subtype C HIV-1 clinical isolate. We employed intracellular homologous recombination
120 (IHR) to produce the recombinant virus. Since the viral swarm generated by IHR did

not show efficient replication in PtM primary cells, we conducted *in vitro* serial passages of the virus. Thus, we successfully generated a viral swarm that exhibited an enhanced replication capacity in PtM cells and established infection in PtMs with high peak viremia comparable to the currently available monkey-tropic HIV-1 derivatives.

Results

Generation of a new HIV-1mt carrying CCR5-tropic subtype C Env through IHR

We employed IHR to generate recombinant viruses (Fujita et al., 2013). First, we prepared DNA fragments by polymerase chain reaction (PCR) amplification of a region spanning the 5′ long terminal repeat (LTR) to upstream of the V1/V2 region in *env* (nucleotide positions 1–6784 based on HXB2 numbering; accession number: K03455) using the plasmid DNA template encoding the full-length NL-DT5R proviral genome (fragment I in Fig. 1A). This fragment encodes a CypA-binding motif derived from the corresponding sequence of SIVmac239 to evade restriction from macaque TRIM5α, and the entire SIVmac239 *vif* gene to counteract the macaque APOBEC3G. Second, a region spanning the *vpr* gene to the R region of the 3′ LTR (nucleotide positions 5558–9625 based on HXB2 numbering) was amplified from the HIV-1 97ZA012 strain (fragment II in Fig. 1B). To increase the possibility to obtain a virus that can replicate in monkeys well, we thought that it was better to generate swarm viruses having variation without cloning. Resultant recombinant virus might fail to replicate normally if recombination occurred between fragments I and II that resulted in the 5′ LTR of

141 subtype B and the 3′ LTR of subtype C. The discordance of the 3′ and 5′ LTR may
142 disrupt successful translocation of the minus strand strong stop DNA to the plus strand
143 genomic RNA during reverse transcription (Goff, 2007). To match the sequence of the
144 3′ LTR to that of the 5′ LTR, we prepared a third DNA fragment encoding a region
145 spanning the 5′ LTR to the middle of *gag* (nucleotide positions 1–1433 based on HXB2
146 numbering) from the proviral DNA extracted from HIV-1 97ZA012-infected cells
147 (fragment III in Fig. 1B). Fragments I and II had an overlapping region between the
148 initiation of *vpr* to upstream of the *env* V1/V2 region, and fragments I and III had an
149 overlapping region between the 5′ LTR to upstream of the CypA-binding site.

150 These amplified DNA fragments (fragments I, II and III) were co-transfected into
151 C8166-CCR5 cells that are permissive to CCR5-tropic HIV-1. On day 8
152 post-transfection, we observed the formation of virus-induced cytopathic effects (CPEs),
153 indicating the generation of replication-competent recombinant virus. The new
154 recombinant virus was isolated and designated HIV-1mt ZA012-P0.

155 To determine the genomic organization of HIV-1mt ZA012-P0, we subjected the
156 viral RNA isolated from the culture supernatant to direct sequencing. We found that the

157 virus carried sequences of the U5 region of the 5′ LTR, *gag*, *pol* and *vif* derived from
158 NL-DT5R and sequences of 3′ half of *env*, *nef*, and R and the U3 region of the 3′ LTR
159 derived from 97ZA012 (Fig. 1C). First, the recombination breakpoint derived from
160 fragments I and III was found to be located within the junction between the U5 and R
161 region of the 5′ LTR (nucleotide positions 551–605 based on HXB2 numbering).
162 However, additional recombination breakpoints between fragments I and II, encoding
163 the *vpr-env* region, were not identified due to multiple peaks at the same locations in the
164 analyzed sequence chromatograms. This result suggested that HIV-1mt ZA012-P0
165 represented a swarm that might contain several variants with various recombination
166 breakpoints.
167
168 **Increased replication competence of HIV-1mt ZA012 through long-term *in vitro***
169 **passage in CD8$^+$ cell-depleted pig-tailed macaque peripheral blood mononuclear**
170 **cells (PBMCs).**
171 We subsequently determined whether HIV-1mt ZA012-P0 replicates in CD8$^+$
172 cell-depleted pig-tailed macaque peripheral blood mononuclear cells (PtM PBMCs), in

which the parental NL-DT5R replicated as described previously (Kamada et al., 2006). HIV-1mt ZA012-P0 from the culture supernatant of C8166-CCR5 was used to spinoculate $CD8^+$ cell-depleted PtM PBMCs, and the virion-associated reverse transcriptase (RT) activity was monitored in the culture supernatant (Fig. 2); however, no RT activity was detected in the culture supernatant after passage 1 (Fig. 2).

Next we carried out *in vitro* serial passages to improve the replication competence of the virus as observed in the cases of HIV-1 (Freed and Martin, 1996; Willey et al., 1988). Infected cells were co-cultured with freshly prepared $CD8^+$ cell-depleted PtM PBMCs every 1 or 2 weeks. Although detectable RT activity was not observed during 10 successive passages (passage 1–10), a low level of viral replication was confirmed by the CPEs of C8166-CCR5 cells co-cultured with PBMCs taken from the passage (data not shown). A detectable peak of viral replication (319 cpm/μL) was observed at 115 days after the first inoculation (passage 11), and replication was maintained following passages, eventually resulting in enhanced replication in PtM PBMCs (1900 cpm/μL in passage 19). The resultant virus, isolated from the culture supernatant of passage 19, was designated HIV-1mt ZA012-P19.

189 To evaluate the replication capacity of the virus, the replication kinetics of HIV-1mt
190 ZA012-P19 were compared to those of the parental NL-DT5R and HIV-1mt ZA012-P0.
191 Each viral stock was normalized by the number of infectious units per cell (in this case,
192 a multiplicity of infection (MOI) of 0.1) and used to inoculate $CD8^+$ cell-depleted PtM
193 PBMCs isolated from two donor monkeys; virion-associated RT activity in the culture
194 supernatant was monitored daily (Fig. 3). Although HIV-1mt ZA012-P19 exhibited a
195 lower level of viral replication compared to that of SIVmac239, the virus showed more
196 efficient replication than NL-DT5R and HIV-1mt ZA012-P0 in cells from both animals.
197 Therefore, we successfully improved the replication capacity of the new HIV-1mt in
198 PtM PBMCs by *in vitro* passaging.
199
200 **Sequence analysis of HIV-1mt ZA012-P0 and ZA012-P19**
201 It is likely that HIV-1mt ZA012-P0 acquired genetic changes and evolved to HIV-1mt
202 ZA012-P19 through the serial passages in PtM PBMCs. To compare the genomic
203 sequence of these viruses, we first performed single genome amplification (SGA) of
204 viral RNA isolated from the culture supernatant to determine the nucleic acid sequences

of the *vpr-env* region (nucleotide positions 5559–8795 based on HXB2) of HIV-1mt ZA012-P0. Subsequently, we identified the sequence of the region containing the expected recombination breakpoints generated by IHR between fragments I and II. Genetic analysis of 17 SGA clones revealed that these sequences had NL-DT5R sequences in the 5′ end and HIV-1 97ZA012 sequences in the 3′ end, with seven different recombination breakpoints in the region (Fig. 4). One recombination breakpoint was detected at nucleotide positions 178–187 of the *vpr* gene in 1/17 SGA sequences (5736–5745 in HXB2 numbering, recombination type R1) with 10 identical base pairs between NL-DT5R and 97ZA012. In addition to R1, we identified the following recombination types: the *vpr* gene in 3/17 SGA sequences (5760–5767; R2), the initiation of *tat* in 2/17 SGA sequences, (5821–5839; R3), the end of the *vpr* gene in 1/17 SGA sequence (5852–5865; R4), the initiation of *rev* in 6/17 SGA sequences (5960–6000; R5), the end of the *vpu* gene in 1/17 SGA sequence (6357–6392; R6) and the upstream of V1/V2 of the *env* gene in 3/17 SGA sequences (6467–6491; R7). These results suggest that homologous recombination occurs in various sites with homologous sequences.

221 Next, seven SGA sequences were amplified from viral RNA isolated from the
222 culture supernatant of PtM PBMCs infected with HIV-1mt ZA012-P19, and nucleotide
223 sequences and recombination breakpoints were determined in the same manner.
224 Unexpectedly, all the sequences of HIV-1mt ZA012-P19 had three recombination
225 breakpoints in the region from the *vpr* to *env* genes (recombination type R8 in Fig. 4).
226 The first breakpoint was located in the *vpr* gene (5760–5767), the second was located in
227 the *vpu* gene (6194–6213), and the third was located in *env* (6467–6491) with the
228 N-terminal portion of C1 region from NL4-3 sequence. Although the pattern of
229 recombination breakpoint of the virus differed from those of HIV-1mt ZA012-P0, the
230 first and third recombination breakpoints were identical to the recombination type of R2
231 and R7, respectively (Fig. 4). It is likely that HIV-1mt ZA012-P19 was generated from
232 further recombination events that occurred in the middle of the *vpu* gene (6194–6213)
233 between recombination type R2 and R7 of HIV-1mt ZA012-P0.

234 It is conceivable that the genome of HIV-1mt ZA012-P19 acquired several amino
235 acid mutations associated with the enhanced replication in PtM PBMCs. Compared with
236 the deduced amino acid sequences in HIV-1mt ZA012-P0, HIV-1mt ZA012-P19

237 acquired substitutions from Lys to Arg at amino acid position 432 in Pol-RT and Asp to
238 Glu at position 232 in Pol-IN that were in the NL-DT5R backbone. In addition, an
239 amino acid substitution from Phe to Ser at 139 in Nef was found in
240 HIV-1mt ZA012-P19 compared to 17 SGA sequences derived from HIV-1mt
241 ZA012-P0. No nonsynonymous substitutions were identified in Gag and Vif, the
242 proteins responsible for evading TRIM5α and APOBEC3. Around the recombination
243 break points in HIV-1mt ZA012-P19, the vpr and vpu genes keep each open reading
244 frame and do not contain any mutations in the region derived from NL-DT5R,
245 respectively. Furthermore, consensus amino acid sequence of P0 and P19 were also
246 identical in the regions derived from HIV-1 97ZA012, respectively. These facts suggest
247 that recombination was occurred to keep these genes intact.
248
249 **Phylogenetic analysis of *env* genes**
250 It is likely that HIV-1mt ZA012-P0 generated by IHR in human C8166-CCR5 cells was
251 a swarm carrying diverse *env* sequences of the parental HIV-1 97ZA012, which evolved
252 to HIV-1mt ZA012-P19 through *in vitro* passages. To evaluate the *env* variants selected

253 in C8166-CCR5 cells or primary PtM cells, we determined 22 sequences of HIV-1
254 97ZA012, 17 sequences of HIV-1mt ZA012-P0 and seven sequences of HIV-1mt
255 ZA012-P19 from SGA. Next, we conducted a phylogenetic analysis of the nucleotide
256 sequences of the 3′ terminal 2361 bp of each viral *env* derived from HIV-1 97ZA012
257 and shared by all variants of HIV-1mt ZA012-P0 and -P19 (Fig. 5). These sequences
258 were divided into two clusters: the larger cluster included 19 sequences of HIV-1
259 97ZA012, 8 sequences of HIV-1mt ZA012-P0 and 7 sequences of HIV-1mt
260 ZA012-P19; and the smaller cluster included 3 sequences of HIV-1 97ZA012 and 9
261 sequences of HIV-1mt ZA012-P0. Recombination types R2, R3, R5 and R7 (Figure 4)
262 were intermingled among the sequences of the two groups, suggesting that homologous
263 recombination could occur in various *env* templates.

264 To compare the genetic diversity of *env* in these viruses, we computed the mean of
265 all pair-wise distances between any two viral *env* sequences in each of the viruses. The
266 computed diversity of *env* in HIV-1mt ZA012-P0 was 0.0038 ± 0.0025 (± standard
267 deviation, SD), which was significantly lower than that in the parental HIV-1 97ZA012
268 (0.0044 ± 0.0021; $p < 0.05$). The computed diversity of HIV-1mt ZA012-P19 *env* was

269 0.0012 ± 0.00078, which showed significantly lower variation compared to HIV-1mt
270 ZA012-P0 ($p < 0.0001$).
271
272 **Co-receptor usage of HIV-1mt ZA012-P19**
273 To characterize co-receptor usage of HIV-1mt ZA012-P19 after long-term *in vitro*
274 passage, we conducted an entry assay using TZM-bl cells with small molecule
275 antagonists (Fig. 6). Viral infectivity of the CXCR4-tropic virus (NL4-3) was reduced
276 in the presence of an increasing amount of the CXCR4 inhibitor, AMD3100, but was
277 not affected by the CCR5 inhibitor, AD101. In contrast, the CCR5-tropic virus,
278 SIVmac239, was inhibited in the presence of an increasing amount of AD101 but not by
279 AMD3100. Similar to the results using SIVmac239, HIV-1mt ZA012-P19 exhibited
280 sensitivity to inhibition by AD101 but resistance to AMD3100, indicating that the virus
281 maintained its CCR5-tropism after the serial passage.
282
283 **Replication of HIV-1mt ZA012 in pig-tailed macaques**
284 Since HIV-1mt ZA012-P19 utilized CCR5 as a co-receptor and exhibited increased

285 infectivity to primary cells of PtMs, we next assessed the *in vivo* replication capacity of
286 the virus by experimental infection of PtMs. Two PtMs were inoculated intravenously
287 with 1.0×10^5 $TCID_{50}$ of the HIV-1mt prepared in PtM PBMCs, and plasma viral RNA
288 burdens and the numbers of circulating $CD4^+$ T-lymphocytes were monitored
289 periodically (Fig. 7A). Plasma viral RNA loads in PtM01 peaked (1.0×10^6 copies/mL)
290 at 2 week post-infection (wpi) and declined thereafter to levels below the detection limit
291 at 8 wpi. PtM02 exhibited a peak plasma viral RNA burden (2.3×10^6 copies/mL) at 1.5
292 wpi and maintained more than 1×10^4 copies/mL by 9 wpi, but the viral load declined
293 to levels below the detection limit at 16 wpi. The numbers of $CD4^+$ T-lymphocytes in
294 the circulation in both animals were not affected (Fig. 7B). Furthermore, we analyzed
295 naive and memory populations of CD4+ T cells and no preferential depletion of
296 circulating memory CD4+ T-lymphocyte was observed (data not shown).
297

297 **Discussion**

298 In this study, we used IHR to generate a new HIV-1mt carrying *env* from the
299 CCR5-tropic subtype C HIV-1 clinical isolate. This recombination method has been
300 used to generate infectious HIV-1 or SHIV by joining two linear DNAs in regions with
301 completely identical sequences (Chen et al., 2000; Kalyanaraman et al., 1988; Kellam
302 and Larder, 1994; Luciw et al., 1995; Srinivasan et al., 1989; Velpandi et al., 1991).
303 Recently, we applied IHR to generate a replication-competent SHIV carrying subtype C
304 *env* that was inserted within the *env* sequence of subtype B (Fujita et al., 2013). Here,
305 we utilized the same method to generate HIV-1mt by replacing a coding sequence
306 region from subtype B with that of a primary isolate of subtype C and investigated
307 recombination breakpoints in detail by analyzing the sequences of the resultant viruses.
308 We found seven variants with different recombination breakpoints that were located
309 within overlapped sequences between fragments I and II. These variants were selected
310 as replication-competent virus in C8166-CCR5 cells that maintained their variability,
311 suggesting that IHR events occur frequently in cells co-transfected with DNA fragments.
312 In addition, it appears that the length of identical sequence of as short as 8 bp is

313 sufficient for IHR (recombination type R2 in Fig. 4). Furthermore, IHR is suggested to
314 occur between various DNA templates, based on the phylogenetic analysis results that
315 indicated intermingled types of recombination breakpoints among different *env*
316 sequences.

317 To develop a virus that efficiently infects monkey cells, it is important to choose an
318 *env* that mediates efficient entry to macaque cells. The Env proteins in most A–D
319 subtypes of HIV-1 clinical isolates from infected individuals during the acute phase of
320 infection do not mediate efficient entry using macaque CD4 receptors (Humes et al.,
321 2012). In a preliminary experiment in C8166-CCR5 cells, we generated five strains of
322 replication-competent HIV-1mt carrying *env* from subtype C HIV-1 clinical isolates,
323 including 97ZA012, but only three were infectious to PtM cells (data not shown). The
324 generation of SHIV 97ZA012 that can establish infection in rhesus macaques as
325 described previously (Fujita et al., 2013) also suggested that Env of HIV-1 97ZA012
326 can generate recombinant viruses that are infectious to macaque cells.

327 The serial passage of HIV-1mt ZA012-P0 through PtM PBMCs resulted in the loss
328 of variants with recombination breakpoints and led to the emergence of HIV-1mt

329 ZA012-P19 variants with shared uniform mosaic breakpoints not detected before the
330 passage (Fig. 4). It is possible that recombination type R8 was generated through
331 additional recombination events within homologous sequences in the *vpu* region
332 between variants with recombination type R2 and R7 because recombinant breakpoints
333 located on *vpr* and *env* regions of the virus were identical to that of R2 and R7,
334 respectively. This possibility of recombination between R2 and R7 is also supported by
335 the previous finding that the AAAAA tract within the putative site of recombination is a
336 recombination hotspot during reverse transcription because the sequence facilitates
337 template switching by pausing and dissociation of reverse transcriptase and results in
338 frequent recombination (Quinones-Mateu et al., 2002).

339 HIV-1mt ZA012-P19 acquired three amino acid substitutions (K432R of Pol-RT,
340 D232E of Pol-IN and F138S of Nef) through serial passages in PtM PBMCs, but the
341 biological significance of these mutations remains undetermined. It has been reported
342 previously that two amino acid substitutions (N222K and V234I) in the C-terminus of
343 Pol-IN of NL4-3 could augment replication of HIV-1mt in cynomolgus macaque
344 HSC-F and human MT4/CCR5 cells (Nomaguchi et al., 2013). A D232E mutation

observed in this study was positioned near these two residues, which might be associated with increased replication in primate cells.

HIV-1mt ZA012 established infection in PtMs with the peak viremia reaching 1.0–2.3 × 10^6 copies/mL at 1.5 or 2 wpi (Fig. 7). In contrast, NL-DT5R exhibited low levels of replication in PtMs (at most 3.5 × 10^4 copies/mL at peak viremia) regardless of $CD8^+$ cell-depletion, as described previously (Igarashi et al., 2007). Plasma viral RNA load at peak viremia in HSIV-vif infected newborn PtMs showed 0.5–1.0 × 10^5 copies/mL (Thippeshappa et al., 2011). The highest peak viral level has been achieved by stHIV-1 infection of PtMs, reaching 1.0 × 10^5–10^6 copies/mL at the peak (Hatziioannou et al., 2009). Although HIV-1mt ZA012 failed to persist its replication over 10 weeks, the replication capacity of the virus in the acute phase appeared to be comparable to or greater than known monkey-tropic HIV-1 isolates. The caveat is that HIV-1mt ZA012 was obtained through “autologous” cell passage.

The derivative of NL-DT5R was designed to counteract or evade restrictions by macaque TRIM5α and APOBEC3G but not by interferon (IFN)-stimulated genes (ISGs). One of the IFNα-inducible host factors, tetherin, inhibits release of viral particles from

361 infected cells (Neil et al., 2008). HIV-1 Vpu is able to counteract human tetherin
362 activity but fails to downregulate this activity in macaque (Jia et al., 2009). On the other
363 hand, unlike HIV-1 HXB2 or NL4-3, some strains of HIV-1 appear to antagonize
364 macaque tetherin by its N-terminal transmembrane (TM) domain of Vpu (Shingai et al.,
365 2011). It has been reported that replication of monkey-tropic HIV-1 could be controlled
366 in macaque lymphocytes treated with IFN-α (Bitzegeio et al., 2013; Thippeshappa et al.,
367 2013). Further investigations are required to determine whether HIV-1mt ZA012-P19
368 that encodes the N-terminal TM domain of Vpu, Env and Nef from subtype C could
369 efficiently replicate in the presence of PtM tetherin or ISGs.

370 We generated the first CCR5-tropic HIV-1mt in the currently available derivatives
371 of HIV-1 that can establish infection in macaques. NL-DT5R, HSIV-vif and stHIV-1
372 are infectious to PtMs, but these viruses are CXCR4 or CXCR4/CCR5 dual tropic.
373 Several monkey-tropic HIV-1 isolates carrying CCR5-tropic *env* have been reported,
374 but the viral replication was less efficient than NL-DT5R (Yamashita et al., 2008). The
375 CCR5-tropic viruses preferentially infect memory $CD4^+$ T-lymphocytes and efficiently
376 replicate in effector sites *in vivo* (*i.e.*, lymphocytes in the lung or gastrointestinal tract)

(Brenchley et al., 2004; Mehandru et al., 2004; Okoye et al., 2007; Picker et al., 2004). Although we characterized co-receptor usage of HIV-1mt ZA012-P19 *in vitro*, further investigation is needed to determine whether the virus behaves similarly to CCR5-tropic HIV-1 isolates in patients *in vivo*.

In this study, we generated a new monkey-tropic HIV-1. The viral swarm HIV-1mt ZA012-P19 carries *env* sequences from CCR5-tropic subtype C HIV-1, and it successfully established infection in PtMs with a high peak viremia comparable or greater than the monkey-tropic HIV-1 strains currently available. Although the monkey-tropic HIV-1 requires further adaptation to improve its *in vivo* replication capacity, the virus potentially serves as a nonhuman primate model for AIDS, which reproduces infection with currently circulating HIV-1.

388 **Materials and methods**

389 **Cells**

390 293 T cells (DuBridge et al., 1987) were maintained in Dulbecco's Modified Eagle
391 Medium (D-MEM; Wako, Osaka, Japan) supplemented with 10% (vol/vol) fetal bovine
392 serum (FBS; HyClone Laboratories, Logan, UT) and 1 mM L-glutamine. TZM-bl cells
393 (Platt et al., 1998) from the NIH AIDS research and reference reagent program were
394 maintained in D-MEM supplemented with 10% FBS, 1 mM L-glutamine and 1 mM
395 sodium pyruvate. The human T-cell line, C8166-CCR5 (Shimizu et al., 2006) was
396 maintained in Rosewell Park Memorial Institute 1640 medium (RPMI-1640; Invitrogen,
397 Carlsbad, CA) supplemented with 10% FBS. PtM PBMCs from uninfected monkeys
398 were isolated using the ficoll density gradient separation method. For this procedure, a
399 mixture of 95% lymphocyte separation medium (Wako) and 5% phosphate buffered
400 saline (PBS) was used as a separation solution as described previously (Agy et al.,
401 1992; Frumkin et al., 1993). Residual erythrocytes were lysed in ACK lysing buffer
402 (0.15 M NH_4Cl, 1.0 M $KHCO_3$, 0.1 mM EDTA·Na_2). Depletion of $CD8^+$ cells was
403 conducted with the magnetic-activated cell sorting (MACS) system (Miltenyi Biotec,

404 Gladbach, Germany). Briefly, isolated PtM PBMCs were stained with phycoerythrin
405 (PE)-conjugated anti-CD8 antibodies (clone SK1, BD Biosciences, San Jose, CA) and
406 then labeled with anti-PE MicroBeads (Miltenyi Biotec). $CD8^+$ cells were removed
407 using a magnetic column according to the manufacturer's instructions. PBMCs were
408 cultured in RPMI-1640 supplemented with 10% FBS, 2 mM sodium pyruvate, 2 mM
409 L-glutamine, 50 nM 2-mercaptoethanol and 40 μg/mL gentamicin. PBMCs were
410 stimulated with 25 μg/mL Concanavalin A (conA) for 20 h and then cultured in the
411 presence of 160 U/mL human recombinant interleukin-2 (IL-2; Wako).
412
413 **Viruses**
414 A stock of NL-DT5R virus was prepared from C8166-CCR5 cells transfected with a
415 plasmid encoding full-length proviral DNA of NL-DT5R (pNL-DT5R) using the
416 DEAE-Dextran/osmotic shock procedure (Takai and Ohmori, 1990). SIVmac239
417 (Kestler et al., 1988) stock virus was prepared from the culture supernatant of 293 T
418 cells transfected with a plasmid encoding full-length proviral DNA of SIVmac239 with
419 Lipofectamine (Invitrogen). CCR5-tropic subtype C HIV-1 clinical isolates including

420 97ZA012 were obtained from the NIH AIDS research and reference reagent program.

421

422 **Generation of recombinant virus through intracellular homologous recombination**

423 To generate recombinant virus by IHR, overlapping viral genomic DNA fragments were
424 prepared by PCR amplification. A region spanning the 5′ LTR to *env* was amplified
425 from pNL-DT5R (GenBank accession number: AB266485) using the HIV-1-U3-NotI-F
426 forward primer (5′-ATGCGGCCGCTGGAAGGGCTAATTTGGTCCCAAAG-3′;
427 nucleotide positions 1–25 in NL-DT5R, and additional *NotI* site sequences) and the
428 env-2R reverse primer (5′-CACAGAGTGGGGTTAATTTTACAC-3′; nucleotide
429 positions 6761–6784 in NL-DT5R). PCR was conducted with Expand long-range
430 dNTPack (Roche Diagnostic, Basel, Switzerland). PCR conditions were as follows:
431 94ºC for 2 min followed by 10 cycles of 94ºC for 15 sec, 55ºC for 30 sec and 68ºC for 8
432 min, 25 cycles of 94ºC for 15 sec, 55ºC for 30 sec, 68ºC for 8 min, with 20 sec
433 increments at 68°C for each successive cycle and a final elongation period of 68ºC for 7
434 min (fragment I in Fig. 1A). Amplification of a DNA fragment spanning the initiation
435 of *vpr* to the 3′ LTR was derived from subtype C HIV-1 clinical isolates of the HIV-1

97ZA012 strain. Viral RNA was isolated from culture supernatant using a QIAamp viral RNA mini kit (Qiagen, Hilden, Germany). Complementary DNA (cDNA) was synthesized with Super Script III first-strand synthesis SuperMix (Invitrogen) using the OFM19-R reverse primer (5′-AGGCAAGCTTTATTGAGGCTTA-3′; nucleotide positions 9604–9625 based on the HXB2 numbering). PCR amplification of the viral cDNA was conducted using HIV-1vpr-F forward primer (5′-AGATGGAACAAGCCCCAGAAGA-3′; nucleotide positions 5558–5579 in the HXB2 numbering) and OFM19-R reverse primer with the same conditions (fragment II in Fig. 1A). To prepare a fragment spanning the initiation of 5′ LTR to the MA region of *gag,* proviral DNA was extracted from proviral DNA of subtype C HIV-1 isolate-infected C8166-CCR5 cells using DNeasy Blood & Tissue kits (Qiagen). The following amplification was conducted using HIV-1cladeC-U3-NotI-F forward primer (5′-ATGCGGCCGCTGGAAGGGTTAATTTACTCAAGAG-3′; nucleotide positions 1–24 in the HXB2 numbering plus *NotI* site sequences) and the PreSCA-R reverse primer (5′-AATCTATCCCATTCTGCAGC-3′; nucleotide positions 1433–1414 in the HXB2 numbering) (fragment III in Fig. 1A). The PCR products were purified using

452 QIAquick PCR purification kits (Qiagen).

453 Recombinant viruses were generated by means of IHR in the cell. PCR-amplified
454 linear viral DNA fragments were co-transfected into C8166-CCR5 cells by the
455 DEAE-dextran/osmotic shock procedure (Takai and Ohmori, 1990). After transfection,
456 cells were maintained and passaged every 3 days. The culture supernatant was harvested
457 upon observation of virus-induced CPE.

458

459 **Virus titration**

460 The infectious titer of the viruses was defined as the median tissue culture infectious
461 dose ($TCID_{50}$) in TZM-bl cells as described previously (Li et al., 2005). Four-fold,
462 serially diluted viral stock was used to inoculated TZM-bl cells (5,000 cells per 200 μL
463 of growth medium containing DEAE-Dextran at a final concentration of 12.5 μg/mL) in
464 quadruplicate in flat-bottom 96-well plates. After incubation for 48 h at 37°C, the
465 culture supernatant was removed and the cells were treated with 50 μl of Cell lysis
466 solution (Toyo-Inki, Tokyo, Japan) for 15 min at room temperature with shaking. Then,
467 30 μl of the cell lysate were transferred to F96 MicroWell plates (Thermo Fisher

468 Scientific, Roskilde, Denmark), and the relative luminescence units (RLU) after adding
469 50 μl of luciferase substrate (PicaGene, Toyo-Inki) to each well was determined using a
470 microplate reader (Mithrus LB940, Berthold Technologies, Bad Wildbad, Germany).
471 Viral infectivity was measured in RLUs, and positive wells were defined as RLU > 2 ×
472 background. The $TCID_{50}$ was calculated as described previously (Reed and Muench,
473 1938).
474
475 **Viral growth kinetics in pig-tailed macaque PBMCs**
476 PtM PBMCs were isolated from two uninfected animals and $CD8^+$ cells were depleted
477 as described above. Two days after stimulation with Concanavarin A (25 μg/ml), 2.5 ×
478 10^5 cells of $CD8^+$ cells-depleted PtM PBMCs were inoculated with 2.5×10^4 $TCID_{50}$ of
479 viral stocks by spinoculation (O'Doherty et al., 2000) at 1,200 × g for 1 h at room
480 temperature. After washing with PBS, the infected cells in 200 μL of culture medium
481 were cultured in round-bottom 96-well plates at 37°C. The upper 150 μl of culture
482 supernatant without aspirating cells in the bottom of the well was exchanged with fresh
483 medium everyday. The harvested supernatant was stored at –20°C prior to measure the

activity of RT associated with virions.

RT assay

The virion-associated RT activity in culture supernatant was monitored as described previously (Willey et al., 1988). Briefly, 6 μL of culture supernatant were combined with 30 μL of RT reaction cocktail [50 mM Tris-HCl, 75 mM KCl, 10 mM dithiothreitol, 4.95 mM $MgCl_2$, 10 mg/mL polyA RNA, 5 mg/mL oligo-dT_{20}, 0.05% NP40] and 1.66×10^4 Becquerel equivalent α^{32}P-dTTP (PerkinElmer, Waltham, Massachusetts, USA) and incubated at 37ºC for 2 h with gentle agitation. Next, 3 μL of incubated mixture were blotted onto DE81 ion exchange cellulose paper (GE healthcare, Buckinghamshire, UK). After four washes with 2× saline sodium citrate (SSC), the residual radioactivity from synthesized DNA was counted using a liquid scintillation counter.

Single genome amplification (SGA)

SGA of the region spanning the initiation region of *vpr* to the end of the *env* gene was

500 conducted as described previously (Salazar-Gonzalez et al., 2008). Synthesized viral
501 cDNA was endpoint diluted and then subjected to nested-PCR. First-round PCR was
502 conducted with KOD-FX (TOYOBO, Osaka, Japan) in a total of 20 μL of reaction
503 mixture, using the SGA-16F forward primer
504 (5′-TGCAGCAGAGTAATCTTCCCACTACAGG-3′; nucleotide positions 5260–5283
505 in NL-DT5R) and the SGA-OFM19R reverse primer
506 (5′-AGGCAAGCTTTATTGAGGCTTAAGCAGTGG-3′; 9771–9800 in NL-DT5R).
507 The first-round PCR conditions were as follows: 94°C for 2 min, followed by 35 cycles
508 of 98°C for 10 sec, 63°C for 30 sec and 68°C for 5 min. Second-round PCR was
509 performed using 1 μL of the first-round PCR product using the SGA-17F forward
510 primer (5′-AGAAGAGACAATAGGAGAGGCCTTCGAATG-3′; 5610–5639 in
511 NL-DT5R) and the SGA-2.5R reverse primer
512 (5′-AAAGCAGCTGCTTATATGCAGCATCTGAGG-3′; 9673–9702 in NL-DT5R).
513 The second-round PCR conditions were the same as those in the first-round PCR.
514 Amplification of the target sequence was confirmed with agarose gel electrophoresis.
515 According to a Poisson distribution, when a positive ratio of amplification from diluted

516 cDNA is < 30% in multiple replicate PCR reactions, the amplicons are predicted to be
517 amplified from one-copy of template with the probability of > 80%. The single genome
518 amplicons were purified before sequence analysis.
519
520 **Genomic analysis**
521 Sequence analysis was performed using the BigDye terminator v. 3.1 cycle sequencing
522 kit (Applied Biosystems, Foster City, CA) and the ABI PRISM 3130xl genetic analyzer
523 (Applied Biosystems). The 3′-terminal 2,304 nucleotide sequences of *env* were aligned
524 using the Clustal X software (Thompson et al., 1997). A neighbor-joining phylogenetic
525 tree (Saitou and Nei, 1987) using Kimura's two-parameter model (Kimura, 1980) was
526 constructed using MEGA 5 software (Tamura et al., 2011), and bootstrap values were
527 computed from 1,000 bootstrap replicates (Felsenstein, 1985). Pair-wise distances
528 between any two nucleic acid sequences of the 3′ terminal 2361 bp of each viral *env*
529 within the parental HIV-1 97ZA012, HIV-1mt ZA012-P0 and HIV-1mt ZA012-P19
530 were calculated with Kimura's two-parameter model (Kimura, 1980) by using MEGA 5
531 software (Tamura et al., 2011). The statistical significance between each viral pair-wise

distance was calculated with Student's t test using GraphPad Prism (San Diego, CA, USA).

Co-receptor usage assay

Employing a previously reported method (Nishimura et al., 2010) with minor modifications, co-receptor usage of viruses was determined using the small molecule antagonists, AD101 (Trkola et al., 2002) provided by Dr. Julie Strizki (Schering-Plough Research Institute, Kenilworth, NJ) and AMD3100 (Sigma-Aldrich, St. Louis, MO) (Donzella et al., 1998). Briefly, freshly trypsinized TZM-bl cells (5,000 cells per 100 µL of growth medium containing DEAE-Dextran at a final concentration of 12.5 µg/mL) were seeded in flat-bottom 96-well plates. The cells were incubated with 50 µL of co-receptor antagonists at final concentrations ranging from 0.1 nM to 1,000 nM for 1 h at 37°C and inoculated with 100 $TCID_{50}$ of replication-competent virus in triplicate. After incubation for 48 h at 37°C, luciferase activity was measured, and the percent infectivity relative to that measured in mock-treated wells was determined.

548 **Experimental infection of pig-tailed macaques with HIV-1mt ZA012**

549 HIV-1mt ZA012 challenge stock was prepared from culture supernatant of PtM PBMCs
550 infected with HIV-1mt ZA012-P19. The virus was titrated with PtM PBMCs as
551 described previously (Fujita et al., 2013). Two pig-tailed macaques, PtM01 and PtM02
552 aged 7 and 6 years, respectively, were intravenously inoculated with 1.0×10^5 $TCID_{50}$
553 of HIV-1mt ZA012. Plasma viral RNA loads were measured with TaqMan real time
554 RT-PCR as described previously (Miyake et al., 2006) with minor modifications;
555 RT-PCR was conducted for HIV-1 *vpr* amplification using the NM3rNvpr-F forward
556 primer (5′-CAGAAGACCAAGGGCCACAG-3′) and NM3rNvpr-R reverse primer
557 (5′-GTCTAACAGCTTCACTCTTAAGTTCCTCT-3′). PCR products were detected
558 with a labeled probe, NM3rNvpr-T (5′-Fam-
559 AGGGAGCCATACAATGAATGGACACT-Tamra-3′; Perkin Elmer). Animal
560 experiments were conducted in the biosafety level 3 animal facility, in compliance with
561 institutional regulations approved by the Committee for Experimental Use of
562 Nonhuman Primates of the Institute for Virus Research, Kyoto University, Kyoto,
563 Japan.

564

565 **Flow cytometry**

566 To enumerate $CD4^+$ T-lymphocytes, and memory and naïve $CD4^+$ T-lymphocytes,
567 whole blood samples were stained with fluorescently labeled mouse monoclonal
568 antibodies. Anti-CD3 (clone SP34-2) conjugated with Pacific Blue, anti-CD4 (clone
569 L200) conjugated with PerCP-Cy5.5, anti-CD8 (clone SK1) conjugated with APC-Cy7,
570 anti-CD20 (clone L27) conjugated with FITC and anti-CD95 (clone DX2) conjugated
571 with APC were purchased from BD Biosciences, and anti-CD28 (clone CD28.2)
572 conjugated with PE was purchased from eBioscience (San Diego, CA).
573 $CD28^{high}CD95^{low}CD4^+$ or $CD28^{high/low}CD95^{high}CD4^+$ T-cell subsets were considered as
574 naïve or memory $CD4^+$ T-lymphocytes, respectively (Pitcher et al., 2002). The absolute
575 number of lymphocytes in the blood was determined using an automated hematology
576 analyzer, KX-21 (Sysmex, Kobe, Japan).

577

577 **Acknowledgements**

578 The authors thank Akio Adachi for providing plasmid DNA encoding the full-length
579 sequence of NL-DT5R; Drs. Julie Strizki and Paul Zavodny of the Schering-Plough
580 Research Institute, Kenilworth, NJ, USA, for providing AD101; the NIH AIDS
581 Research & Reference Reagent Program for providing primary isolates of HIV-1 and
582 TZM-bl cells; Kenta Matsuda for helpful discussion; former and current members of the
583 Igarashi Laboratory for discussion and support with animal procedures and analyses.
584 This work was supported by a Research on HIV/AIDS grant (awarded to T.M. and T.I.,
585 independently) from The Ministry of Health, Labor and Welfare of Japan, and by a
586 Grant-in-Aid for Scientific Research (B) (awarded to T.M. and T.I., independently)
587 from the Japan Society for the Promotion of Science.

588

589

589 **References**

590

591 Agy, M.B., Frumkin, L.R., Corey, L., Coombs, R.W., Wolinsky, S.M., Koehler, J.,
592 Morton, W.R., Katze, M.G., 1992. Infection of Macaca nemestrina by human
593 immunodeficiency virus type-1. Science 257, 103-106.

594 Berthoux, L., Sebastian, S., Sokolskaja, E., Luban, J., 2005. Cyclophilin A is required
595 for TRIM5{alpha}-mediated resistance to HIV-1 in Old World monkey cells.
596 Proceedings of the National Academy of Sciences of the United States of
597 America 102, 14849-14853.

598 Bitzegeio, J., Sampias, M., Bieniasz, P.D., Hatziioannou, T., 2013. Adaptation to the
599 interferon-induced antiviral state by human and simian immunodeficiency
600 viruses. Journal of virology 87, 3549-3560.

601 Brenchley, J.M., Schacker, T.W., Ruff, L.E., Price, D.A., Taylor, J.H., Beilman, G.J.,
602 Nguyen, P.L., Khoruts, A., Larson, M., Haase, A.T., Douek, D.C., 2004. CD4+
603 T cell depletion during all stages of HIV disease occurs predominantly in the
604 gastrointestinal tract. The Journal of experimental medicine 200, 749-759.

605 Brennan, G., Kozyrev, Y., Hu, S.-L., 2008. TRIMCyp expression in Old World
606 primates *Macaca nemestrina* and *Macaca fascicularis*. Proceedings of the
607 National Academy of Sciences of the United States of America 105, 3569–3574.

608 Chen, Z., Huang, Y., Zhao, X., Skulsky, E., Lin, D., Ip, J., Gettie, A., Ho, D.D., 2000.
609 Enhanced infectivity of an R5-tropic simian/human immunodeficiency virus
610 carrying human immunodeficiency virus type 1 subtype C envelope after serial
611 passages in pig-tailed macaques (Macaca nemestrina). Journal of virology 74,
612 6501-6510.

613 Choe, H., Farzan, M., Sun, Y., Sullivan, N., Rollins, B., Ponath, P.D., Wu, L., Mackay,
614 C.R., LaRosa, G., Newman, W., Gerard, N., Gerard, C., Sodroski, J., 1996. The
615 beta-chemokine receptors CCR3 and CCR5 facilitate infection by primary
616 HIV-1 isolates. Cell 85, 1135-1148.

617 Choisy, M., Woelk, C.H., Guegan, J.F., Robertson, D.L., 2004. Comparative study of
618 adaptive molecular evolution in different human immunodeficiency virus groups
619 and subtypes. Journal of virology 78, 1962-1970.

620 Donzella, G.A., Schols, D., Lin, S.W., Este, J.A., Nagashima, K.A., Maddon, P.J.,
621 Allaway, G.P., Sakmar, T.P., Henson, G., De Clercq, E., Moore, J.P., 1998.

622 AMD3100, a small molecule inhibitor of HIV-1 entry via the CXCR4
623 co-receptor. Nature medicine 4, 72-77.
624 Doranz, B.J., Rucker, J., Yi, Y., Smyth, R.J., Samson, M., Peiper, S.C., Parmentier, M.,
625 Collman, R.G., Doms, R.W., 1996. A dual-tropic primary HIV-1 isolate that
626 uses fusin and the beta-chemokine receptors CKR-5, CKR-3, and CKR-2b as
627 fusion cofactors. Cell 85, 1149-1158.
628 DuBridge, R.B., Tang, P., Hsia, H.C., Leong, P.M., Miller, J.H., Calos, M.P., 1987.
629 Analysis of mutation in human cells by using an Epstein-Barr virus shuttle
630 system. Mol Cell Biol 7, 379-387.
631 Felsenstein, J., 1985. Confidence limits on phylogenies: an approach using the bootstrap.
632 Evolution 39, 783–791.
633 Feng, Y., Broder, C.C., Kennedy, P.E., Berger, E.A., 1996. HIV-1 entry cofactor:
634 functional cDNA cloning of a seven-transmembrane, G protein-coupled receptor.
635 Science 272, 872-877.
636 Freed, E.O., Martin, M.A., 1996. Domains of the human immunodeficiency virus type 1
637 matrix and gp41 cytoplasmic tail required for envelope incorporation into
638 virions. Journal of virology 70, 341-351.
639 Frumkin, L.R., Agy, M.B., Coombs, R.W., Panther, L., Morton, W.R., Koehler, J.,
640 Florey, M.J., Dragavon, J., Schmidt, A., Katze, M.G., et al., 1993. Acute
641 infection of Macaca nemestrina by human immunodeficiency virus type 1.
642 Virology 195, 422-431.
643 Fujita, Y., Otsuki, H., Watanabe, Y., Yasui, M., Kobayashi, T., Miura, T., Igarashi, T.,
644 2013. Generation of a replication-competent chimeric simian-human
645 immunodeficiency virus carrying env from subtype C clinical isolate through
646 intracellular homologous recombination. Virology 436, 100-111.
647 Gaschen, B., Taylor, J., Yusim, K., Foley, B., Gao, F., Lang, D., Novitsky, V., Haynes,
648 B., Hahn, B.H., Bhattacharya, T., Korber, B., 2002. Diversity considerations in
649 HIV-1 vaccine selection. Science 296, 2354-2360.
650 Gibbs, R.A., Rogers, J., Katze, M.G., Bumgarner, R., Weinstock, G.M., Mardis, E.R.,
651 Remington, K.A., Strausberg, R.L., Venter, J.C., Wilson, R.K., Batzer, M.A.,
652 Bustamante, C.D., Eichler, E.E., Hahn, M.W., Hardison, R.C., Makova, K.D.,
653 Miller, W., Milosavljevic, A., Palermo, R.E., Siepel, A., Sikela, J.M., Attaway,
654 T., Bell, S., Bernard, K.E., Buhay, C.J., Chandrabose, M.N., Dao, M., Davis, C.,

655 Delehaunty, K.D., Ding, Y., Dinh, H.H., Dugan-Rocha, S., Fulton, L.A., Gabisi,
656 R.A., Garner, T.T., Godfrey, J., Hawes, A.C., Hernandez, J., Hines, S., Holder,
657 M., Hume, J., Jhangiani, S.N., Joshi, V., Khan, Z.M., Kirkness, E.F., Cree, A.,
658 Fowler, R.G., Lee, S., Lewis, L.R., Li, Z., Liu, Y.S., Moore, S.M., Muzny, D.,
659 Nazareth, L.V., Ngo, D.N., Okwuonu, G.O., Pai, G., Parker, D., Paul, H.A.,
660 Pfannkoch, C., Pohl, C.S., Rogers, Y.H., Ruiz, S.J., Sabo, A., Santibanez, J.,
661 Schneider, B.W., Smith, S.M., Sodergren, E., Svatek, A.F., Utterback, T.R.,
662 Vattathil, S., Warren, W., White, C.S., Chinwalla, A.T., Feng, Y., Halpern, A.L.,
663 Hillier, L.W., Huang, X., Minx, P., Nelson, J.O., Pepin, K.H., Qin, X., Sutton,
664 G.G., Venter, E., Walenz, B.P., Wallis, J.W., Worley, K.C., Yang, S.P., Jones,
665 S.M., Marra, M.A., Rocchi, M., Schein, J.E., Baertsch, R., Clarke, L., Csuros,
666 M., Glasscock, J., Harris, R.A., Havlak, P., Jackson, A.R., Jiang, H., Liu, Y.,
667 Messina, D.N., Shen, Y., Song, H.X., Wylie, T., Zhang, L., Birney, E., Han, K.,
668 Konkel, M.K., Lee, J., Smit, A.F., Ullmer, B., Wang, H., Xing, J., Burhans, R.,
669 Cheng, Z., Karro, J.E., Ma, J., Raney, B., She, X., Cox, M.J., Demuth, J.P.,
670 Dumas, L.J., Han, S.G., Hopkins, J., Karimpour-Fard, A., Kim, Y.H., Pollack,
671 J.R., Vinar, T., Addo-Quaye, C., Degenhardt, J., Denby, A., Hubisz, M.J., Indap,
672 A., Kosiol, C., Lahn, B.T., Lawson, H.A., Marklein, A., Nielsen, R., Vallender,
673 E.J., Clark, A.G., Ferguson, B., Hernandez, R.D., Hirani, K., Kehrer-Sawatzki,
674 H., Kolb, J., Patil, S., Pu, L.L., Ren, Y., Smith, D.G., Wheeler, D.A., Schenck, I.,
675 Ball, E.V., Chen, R., Cooper, D.N., Giardine, B., Hsu, F., Kent, W.J., Lesk, A.,
676 Nelson, D.L., O'Brien W, E., Prufer, K., Stenson, P.D., Wallace, J.C., Ke, H.,
677 Liu, X.M., Wang, P., Xiang, A.P., Yang, F., Barber, G.P., Haussler, D.,
678 Karolchik, D., Kern, A.D., Kuhn, R.M., Smith, K.E., Zwieg, A.S., 2007.
679 Evolutionary and biomedical insights from the rhesus macaque genome. Science
680 316, 222-234.

681 Gnanakaran, S., Lang, D., Daniels, M., Bhattacharya, T., Derdeyn, C.A., Korber, B.,
682 2007. Clade-specific differences between human immunodeficiency virus type 1
683 clades B and C: diversity and correlations in C3-V4 regions of gp120. Journal of
684 virology 81, 4886-4891.

685 Goff, S.P., 2007. Retroviridae: The Retroviruses and Their Replication, in: Knipe, D.M.,
686 Howley, P.M. (Eds.), Fields Virology, 5th Edition. Lippincott Williams &
687 Wilkins, Philadelphia, PA.

688 Goulder, P.J., Watkins, D.I., 2004. HIV and SIV CTL escape: implications for vaccine
689 design. Nature reviews. Immunology 4, 630-640.
690 Harouse, J.M., Gettie, A., Tan, R.C.H., Blanchard, J., Cheng-Mayer, C., 1999. Distinct
691 pathogenic sequela in rhesus macaques infected with CCR5 or CXCR4 utilizing
692 SHIVs. Science 284, 816-819.
693 Hatziioannou, T., Ambrose, Z., Chung, N.P., Piatak, M., Jr., Yuan, F., Trubey, C.M.,
694 Coalter, V., Kiser, R., Schneider, D., Smedley, J., Pung, R., Gathuka, M., Estes,
695 J.D., Veazey, R.S., KewalRamani, V.N., Lifson, J.D., Bieniasz, P.D., 2009. A
696 macaque model of HIV-1 infection. Proceedings of the National Academy of
697 Sciences of the United States of America 106, 4425-4429.
698 Hatziioannou, T., Princiotta, M., Piatak, M., Yuan, F., Zhang, F., Lifson, J.D., Bieniasz,
699 P.D., 2006. Generation of simian-tropic HIV-1 by restriction factor evasion.
700 Science 314, 95.
701 Hemelaar, J., 2012. The origin and diversity of the HIV-1 pandemic. Trends in
702 molecular medicine 18, 182-192.
703 Humes, D., Emery, S., Laws, E., Overbaugh, J., 2012. A species-specific amino acid
704 difference in the macaque CD4 receptor restricts replication by global
705 circulating HIV-1 variants representing viruses from recent infection. Journal of
706 virology 86, 12472-12483.
707 Igarashi, T., Iyengar, R., Byrum, R.A., Buckler-White, A., Dewar, R.L., Buckler, C.E.,
708 Lane, H.C., Kamada, K., Adachi, A., Martin, M.A., 2007. Human
709 immunodeficiency virus type 1 derivative with 7% simian immunodeficiency
710 virus genetic content is able to establish infections in pig-tailed macaques.
711 Journal of virology 81, 11549-11552.
712 Javaherian, K., Langlois, A.J., Schmidt, S., Kaufmann, M., Cates, N., Langedijk, J.P.,
713 Meloen, R.H., Desrosiers, R.C., Burns, D.P., Bolognesi, D.P., et al., 1992. The
714 principal neutralization determinant of simian immunodeficiency virus differs
715 from that of human immunodeficiency virus type 1. Proceedings of the National
716 Academy of Sciences of the United States of America 89, 1418-1422.
717 Jia, B., Serra-Moreno, R., Neidermyer, W., Rahmberg, A., Mackey, J., Fofana, I.B.,
718 Johnson, W.E., Westmoreland, S., Evans, D.T., 2009. Species-specific activity
719 of SIV Nef and HIV-1 Vpu in overcoming restriction by tetherin/BST2. PLoS
720 pathogens 5, e1000429.

721 Kalyanaraman, S., Jannoun-Nasr, R., York, D., Luciw, P.A., Robinson, R., Srinivasan,
722 A., 1988. Homologous recombination between human immunodeficiency viral
723 DNAs in cultured human cells: analysis of the factors influencing recombination.
724 Biochemical and biophysical research communications 157, 1051-1060.
725 Kamada, K., Igarashi, T., Martin, M.A., Khamsri, B., Hatcho, K., Yamashita, T., Fujita,
726 M., Uchiyama, T., Adachi, A., 2006. Generation of HIV-1 derivatives that
727 productively infect macaque monkey lymphoid cells. Proceedings of the
728 National Academy of Sciences of the United States of America 103,
729 16959-16964.
730 Kanki, P.J., McLane, M.F., King, N.W., Jr., Letvin, N.L., Hunt, R.D., Sehgal, P., Daniel,
731 M.D., Desrosiers, R.C., Essex, M., 1985. Serologic identification and
732 characterization of a macaque T-lymphotropic retrovirus closely related to
733 HTLV-III. Science 228, 1199-1201.
734 Keckesova, Z., Ylinen, L.M., Towers, G.J., 2006. Cyclophilin A renders human
735 immunodeficiency virus type 1 sensitive to Old World monkey but not human
736 TRIM5 alpha antiviral activity. Journal of virology 80, 4683-4690.
737 Kellam, P., Larder, B.A., 1994. Recombinant virus assay: a rapid, phenotypic assay for
738 assessment of drug susceptibility of human immunodeficiency virus type 1
739 isolates. Antimicrobial Agents and Chemotherapy 38, 23-30.
740 Kestler, H.W., 3rd, Li, Y., Naidu, Y.M., Butler, C.V., Ochs, M.F., Jaenel, G., King,
741 N.W., Daniel, M.D., Desrosiers, R.C., 1988. Comparison of simian
742 immunodeficiency virus isolates. Nature 331, 619-622.
743 Kiepiela, P., Ngumbela, K., Thobakgale, C., Ramduth, D., Honeyborne, I., Moodley, E.,
744 Reddy, S., de Pierres, C., Mncube, Z., Mkhwanazi, N., Bishop, K., van der Stok,
745 M., Nair, K., Khan, N., Crawford, H., Payne, R., Leslie, A., Prado, J.,
746 Prendergast, A., Frater, J., McCarthy, N., Brander, C., Learn, G.H., Nickle, D.,
747 Rousseau, C., Coovadia, H., Mullins, J.I., Heckerman, D., Walker, B.D.,
748 Goulder, P., 2007. CD8+ T-cell responses to different HIV proteins have
749 discordant associations with viral load. Nature medicine 13, 46-53.
750 Kimura, M., 1980. A simple method for estimating evolutionary rates of base
751 substitutions through comparative studies of nucleotide sequences. Journal of
752 molecular evolution 16, 111-120.
753 Kuiken, C.L., Foley, B., Guzman, E., Korber, B.T., 1999. Determinants of HIV-1

754 Protein Evolution, in: Crandall, K.A. (Ed.), Molecular Evolution of HIV. Johns
755 Hopkins University Press, Baltimore MD.
756 Li, M., Gao, F., Mascola, J.R., Stamatatos, L., Polonis, V.R., Koutsoukos, M., Voss, G.,
757 Goepfert, P., Gilbert, P., Greene, K.M., Bilska, M., Kothe, D.L.,
758 Salazar-Gonzalez, J.F., Wei, X., Decker, J.M., Hahn, B.H., Montefiori, D.C.,
759 2005. Human immunodeficiency virus type 1 env clones from acute and early
760 subtype B infections for standardized assessments of vaccine-elicited
761 neutralizing antibodies. Journal of virology 79, 10108-10125.
762 Luciw, P.A., Pratt-Lowe, E., Shaw, K.E., Levy, J.A., Cheng-Mayer, C., 1995. Persistent
763 infection of rhesus macaques with T-cell-line-tropic and macrophage-tropic
764 clones of simian/human immunodeficiency viruses (SHIV). Proceedings of the
765 National Academy of Sciences of the United States of America 92, 7490-7494.
766 Mariani, R., Chen, D., Schrofelbauer, B., Navarro, F., Konig, R., Bollman, B., Munk, C.,
767 Nymark-McMahon, H., Landau, N.R., 2003. Species-specific exclusion of
768 APOBEC3G from HIV-1 virions by Vif. Cell 114, 21-31.
769 Mehandru, S., Poles, M.A., Tenner-Racz, K., Horowitz, A., Hurley, A., Hogan, C.,
770 Boden, D., Racz, P., Markowitz, M., 2004. Primary HIV-1 infection is
771 associated with preferential depletion of CD4+ T lymphocytes from effector
772 sites in the gastrointestinal tract. The Journal of experimental medicine 200,
773 761-770.
774 Miyake, A., Ibuki, K., Enose, Y., Suzuki, H., Horiuchi, R., Motohara, M., Saito, N.,
775 Nakasone, T., Honda, M., Watanabe, T., Miura, T., Hayami, M., 2006. Rapid
776 dissemination of a pathogenic simian/human immunodeficiency virus to
777 systemic organs and active replication in lymphoid tissues following intrarectal
778 infection. The Journal of general virology 87, 1311-1320.
779 Moore, P.L., Gray, E.S., Choge, I.A., Ranchobe, N., Mlisana, K., Abdool Karim, S.S.,
780 Williamson, C., Morris, L., 2008. The c3-v4 region is a major target of
781 autologous neutralizing antibodies in human immunodeficiency virus type 1
782 subtype C infection. Journal of virology 82, 1860-1869.
783 Moore, P.L., Ranchobe, N., Lambson, B.E., Gray, E.S., Cave, E., Abrahams, M.R.,
784 Bandawe, G., Mlisana, K., Abdool Karim, S.S., Williamson, C., Morris, L.,
785 2009. Limited neutralizing antibody specificities drive neutralization escape in
786 early HIV-1 subtype C infection. PLoS pathogens 5, e1000598.

787 Murphey-Corb, M., Martin, L.N., Rangan, S.R., Baskin, G.B., Gormus, B.J., Wolf, R.H.,
788 Andes, W.A., West, M., Montelaro, R.C., 1986. Isolation of an
789 HTLV-III-related retrovirus from macaques with simian AIDS and its possible
790 origin in asymptomatic mangabeys. Nature 321, 435-437.
791 Ndung'u, T., Lu, Y., Renjifo, B., Touzjian, N., Kushner, N., Pena-Cruz, V., Novitsky,
792 V.A., Lee, T.H., Essex, M., 2001. Infectious simian/human immunodeficiency
793 virus with human immunodeficiency virus type 1 subtype C from an African
794 isolate: rhesus macaque model. Journal of virology 75, 11417-11425
795 Neil, S., Bieniasz, P., 2009. Human immunodeficiency virus, restriction factors, and
796 interferon. Journal of interferon & cytokine research : the official journal of the
797 International Society for Interferon and Cytokine Research 29, 569-580.
798 Neil, S.J., Zang, T., Bieniasz, P.D., 2008. Tetherin inhibits retrovirus release and is
799 antagonized by HIV-1 Vpu. Nature 451, 425-430.
800 Nishimura, Y., Igarashi, T., Donau, O.K., Buckler-White, A., Buckler, C., Lafont, B.A.,
801 Goeken, R.M., Goldstein, S., Hirsch, V.M., Martin, M.A., 2004. Highly
802 pathogenic SHIVs and SIVs target different CD4+ T cell subsets in rhesus
803 monkeys, explaining their divergent clinical courses. Proceedings of the
804 National Academy of Sciences of the United States of America 101,
805 12324-12329.
806 Nishimura, Y., Shingai, M., Willey, R., Sadjadpour, R., Lee, W.R., Brown, C.R.,
807 Brenchley, J.M., Buckler-White, A., Petros, R., Eckhaus, M., Hoffman, V.,
808 Igarashi, T., Martin, M. A., 2010. Generation of the pathogenic R5-tropic
809 simian/human immunodeficiency virus SHIVAD8 by serial passaging in rhesus
810 macaques. Journal of virology 84, 4769-4781.
811 Nomaguchi, M., Doi, N., Fujiwara, S., Saito, A., Akari, H., Nakayama, E.E., Shioda, T.,
812 Yokoyama, M., Sato, H., Adachi, A., 2013. Systemic biological analysis of the
813 mutations in two distinct HIV-1mt genomes occurred during replication in
814 macaque cells. Microbes and infection / Institut Pasteur 15, 319-328.
815 O'Doherty, U., Swiggard, W.J., Malim, M.H., 2000. Human immunodeficiency virus
816 type 1 spinoculation enhances infection through virus binding. Journal of
817 virology 74, 10074-10080.
818 Okoye, A., Meier-Schellersheim, M., Brenchley, J.M., Hagen, S.I., Walker, J.M.,
819 Rohankhedkar, M., Lum, R., Edgar, J.B., Planer, S.L., Legasse, A., Sylwester,

A.W., Piatak, M., Jr., Lifson, J.D., Maino, V.C., Sodora, D.L., Douek, D.C., Axthelm, M.K., Grossman, Z., Picker, L.J., 2007. Progressive CD4+ central memory T cell decline results in CD4+ effector memory insufficiency and overt disease in chronic SIV infection. The Journal of experimental medicine 204, 2171-2185.

Picker, L.J., Hagen, S.I., Lum, R., Reed-Inderbitzin, E.F., Daly, L.M., Sylwester, A.W., Walker, J.M., Siess, D.C., Piatak, M., Jr., Wang, C., Allison, D.B., Maino, V.C., Lifson, J.D., Kodama, T., Axthelm, M.K., 2004. Insufficient production and tissue delivery of CD4+ memory T cells in rapidly progressive simian immunodeficiency virus infection. The Journal of experimental medicine 200, 1299-1314.

Pitcher, C.J., Hagen, S.I., Walker, J.M., Lum, R., Mitchell, B.L., Maino, V.C., Axthelm, M.K., Picker, L.J., 2002. Development and homeostasis of T cell memory in rhesus macaque. Journal of immunology 168, 29-43.

Platt, E.J., Wehrly, K., Kuhmann, S.E., Chesebro, B., Kabat, D., 1998. Effects of CCR5 and CD4 cell surface concentrations on infections by macrophagetropic isolates of human immunodeficiency virus type 1. Journal of virology 72, 2855-2864.

Quinones-Mateu, M.E., Gao, Y., Ball, S.C., Marozsan, A.J., Abraha, A., Arts, E.J., 2002. In vitro intersubtype recombinants of human immunodeficiency virus type 1: comparison to recent and circulating in vivo recombinant forms. Journal of virology 76, 9600-9613.

Reed, L., J.,, Muench, H., 1938. A simple method of estimating fifty percent endpoints. Am. J. Hyg 27, 493-497.

Reimann, K.A., Li, J.T., Veazey, R., Halloran, M., Park, I.-W., Karlsson, G.B., Sodroski, J., Letvin, N., 1996. A chimeric simian/human immunodeficiency virus expressing a primary patient human immunodeficiency vrus type 1isolate *env* causes an AIDS-like disease after *in vivo* passage in rhesus monkeys. Journal of virology 70, 6922–6928.

Ren, W., Mumbauer, A., Gettie, A., Seaman, M.S., Russell-Lodrigue, K., Blanchard, J., Westmoreland, S., Cheng-Mayer, C., 2013. Generation of lineage-related, mucosally transmissible subtype C R5 simian-human immunodeficiency viruses capable of AIDS development, induction of neurological disease, and coreceptor switching in rhesus macaques. Journal of virology 87, 6137-6149.

853 Saitou, N., Nei, M., 1987. The neighbor-joining method: a new method for
854 reconstructing phylogenetic trees. Molecular biology and evolution 4, 406-425.
855 Salazar-Gonzalez, J.F., Bailes, E., Pham, K.T., Salazar, M.G., Guffey, M.B., Keele,
856 B.F., Derdeyn, C.A., Farmer, P., Hunter, E., Allen, S., Manigart, O., Mulenga, J.,
857 Anderson, J.A., Swanstrom, R., Haynes, B.F., Athreya, G.S., Korber, B.T.,
858 Sharp, P.M., Shaw, G.M., Hahn, B.H., 2008. Deciphering human
859 immunodeficiency virus type 1 transmission and early envelope diversification
860 by single-genome amplification and sequencing. Journal of virology 82,
861 3952-3970.
862 Sheehy, A.M., Gaddis, N.C., Choi, J.D., Malim, M.H., 2002. Isolation of a human gene
863 that inhibits HIV-1 infection and is suppressed by the viral Vif protein. Nature
864 418, 646-650.
865 Shibata, R., Adachi, A., 1992. SIV/HIV recombinants and their use in studying
866 biological properties. AIDS research and human retroviruses 8, 403-409.
867 Shimizu, Y., Okoba, M., Yamazaki, N., Goto, Y., Miura, T., Hayami, M., Hoshino, H.,
868 Haga, T., 2006. Construction and in vitro characterization of a chimeric simian
869 and human immunodeficiency virus with the RANTES gene. Microbes and
870 infection / Institut Pasteur 8, 105-113.
871 Shingai, M., Yoshida, T., Martin, M.A., Strebel, K., 2011. Some human
872 immunodeficiency virus type 1 Vpu proteins are able to antagonize macaque
873 BST-2 in vitro and in vivo: Vpu-negative simian-human immunodeficiency
874 viruses are attenuated in vivo. Journal of virology 85, 9708-9715.
875 Song, R.J., Chenine, A.L., Rasmussen, R.A., Ruprecht, C.R., Mirshahidi, S., Grisson,
876 R.D., Xu, W., Whitney, J.B., Goins, L.M., Ong, H., Li, P.L., Shai-Kobiler, E.,
877 Wang, T., McCann, C.M., Zhang, H., Wood, C., Kankasa, C., Secor, W.E.,
878 McClure, H.M., Strobert, E., Else, J.G., Ruprecht, R.M., 2006. Molecularly
879 cloned SHIV-1157ipd3N4: a highly replication- competent, mucosally
880 transmissible R5 simian-human immunodeficiency virus encoding HIV clade
881 C Env. Journal of virology 80, 8729-8738
882 Srinivasan, A., York, D., Jannoun-Nasr, R., Kalyanaraman, S., Swan, D., Benson, J.,
883 Bohan, C., Luciw, P.A., Schnoll, S., Robinson, R.A., Desai, S.M., Devare, S.G.,
884 1989. Generation of hybrid human immunodeficiency virus by homologous
885 recombination. Proceedings of the National Academy of Sciences of the United

886 States of America 86, 6388-6392.
887 Stremlau, M., Owens, C.M., Perron, M.J., Kiessling, M., Autissier, P., Sodroski, J.,
888 2004. The cytoplasmic body component TRIM5alpha restricts HIV-1 infection
889 in Old World monkeys. Nature 427, 848-853.
890 Stremlau, M., Perron, M., Lee, M., Li, Y., Song, B., Javanbakht, H., Diaz-Griffero, F.,
891 Anderson, D.J., Sundquist, W.I., Sodroski, J., 2006. Specific recognition and
892 accelerated uncoating of retroviral capsids by the TRIM5alpha restriction factor.
893 Proceedings of the National Academy of Sciences of the United States of
894 America 103, 5514-5519.
895 Takai, T., Ohmori, H., 1990. DNA transfection of mouse lymphoid cells by the
896 combination of DEAE-dextran-mediated DNA uptake and osmotic shock
897 procedure. Biochimica et biophysica acta 1048, 105-109.
898 Tamura, K., Peterson, D., Peterson, N., Stecher, G., Nei, M., Kumar, S., 2011. MEGA5:
899 molecular evolutionary genetics analysis using maximum likelihood,
900 evolutionary distance, and maximum parsimony methods. Molecular biology
901 and evolution 28, 2731-2739.
902 Thippeshappa, R., Polacino, P., Yu Kimata, M.T., Siwak, E.B., Anderson, D., Wang,
903 W., Sherwood, L., Arora, R., Wen, M., Zhou, P., Hu, S.L., Kimata, J.T., 2011.
904 Vif substitution enables persistent infection of pig-tailed macaques by human
905 immunodeficiency virus type 1. Journal of virology 85, 3767-3779.
906 Thippeshappa, R., Ruan, H., Wang, W., Zhou, P., Kimata, J.T., 2013. A Variant
907 Macaque-Tropic Human Immunodeficiency Virus Type 1 Is Resistant to Alpha
908 Interferon-Induced Restriction in Pig-Tailed Macaque CD4+ T Cells. Journal of
909 virology 87, 6678-6692.
910 Thompson, J.D., Gibson, T.J., Plewniak, F., Jeanmougin, F., Higgins, D.G., 1997. The
911 CLUSTAL_X windows interface: flexible strategies for multiple sequence
912 alignment aided by quality analysis tools. Nucleic acids research 25, 4876-4882.
913 Trkola, A., Kuhmann, S.E., Strizki, J.M., Maxwell, E., Ketas, T., Morgan, T., Pugach,
914 P., Xu, S., Wojcik, L., Tagat, J., Palani, A., Shapiro, S., Clader, J.W.,
915 McCombie, S., Reyes, G.R., Baroudy, B.M., Moore, J.P., 2002. HIV-1 escape
916 from a small molecule, CCR5-specific entry inhibitor does not involve CXCR4
917 use. Proceedings of the National Academy of Sciences of the United States of
918 America 99, 395-400.

Velpandi, A., Nagashunmugam, T., Murthy, S., Cartas, M., Monken, C., Srinivasan, A., 1991. Generation of hybrid human immunodeficiency virus utilizing the cotransfection method and analysis of cellular tropism. Journal of virology 65, 4847-4852.

Willey, R.L., Smith, D.H., Lasky, L.A., Theodore, T.S., Earl, P.L., Moss, B., Capon, D.J., Martin, M.A., 1988. In vitro mutagenesis identifies a region within the envelope gene of the human immunodeficiency virus that is critical for infectivity. Journal of virology 62, 139-147.

Yamashita, T., Doi, N., Adachi, A., Nomaguchi, M., 2008. Growth ability in simian cells of monkey cell-tropic HIV-1 is greatly affected by downstream region of the vif gene. The journal of medical investigation : JMI 55, 236-240.

932 **Figure Legends**

933 **Fig 1. Schematic representation of the genome organization of human**
934 **immunodeficiency virus (HIV)-1 and monkey-tropic HIV-1 (HIV-1mt).** Genome
935 organizations of NL-DT5R (A), subtype C HIV-1 97Z012 (B) and HIV-1mt ZA012-P0
936 (C) are depicted. The horizontal line represents DNA fragments I, II and III, used for
937 intracellular homologous recombination. Fragment I encodes a region from the 5′ LTR
938 to *env* of NL-DT5R plasmid DNA. Fragment II encodes a region from the initiation of
939 *vpr* to the R region of the 3′ LTR of the HIV-1 97ZA012 strain. Fragment III encodes a
940 region from the 5′ LTR to upstream of the cyclophilin A-binding motif of the virus.
941 Sequences from NL4-3 (open box), HIV-1 97ZA012 (filled box) and the SIVmac239
942 genome (diagonally striped box) are depicted. The gray box in HIV-1mt ZA012-P0
943 represents a gene that was not identified by direct sequence analysis.

944

945 **Fig 2. Improved replication of HIV-1mt ZA012 throughout *in vitro* passages in**
946 **$CD8^+$ cell-depleted PtM peripheral blood mononuclear cells (PBMCs).**
947 HIV-1mt ZA012-P0 was used to spinoculate $CD8^+$ cell-depleted PtM PBMCs, and
948 virion-associated RT activity in the culture supernatant was monitored daily. Some of

949 the infected cells were co-cultured with freshly prepared $CD8^+$ cell-depleted PtM
950 PBMCs. One period of passage was indicated in the shaded grey or white zones. The
951 dotted line indicates data not available.
952
953 **Fig 3. Growth kinetics of HIV-1mt ZA012 in $CD8^+$ cell-depleted depleted PtM**
954 **PBMCs.** Growth kinetics of HIV-1mt ZA012-P0, HIV-1mt ZA012-P19, SIVmac239
955 and NL-DT5R were compared in PBMCs from two PtMs. Each virus was used to
956 spinoculate $CD8^+$ cell-depleted PtM PBMCs (MOI = 0.1 $TCID_{50}$ per cell), and the
957 virion-associated RT activity in the culture supernatant was monitored. The figure
958 shown is representative of four independent experiments.
959
960 **Fig 4. Recombination breakpoints in HIV-1mt ZA012-P0 and ZA012-P19 genomes.**
961 The genome organizations of HIV-1mt ZA012-P0 and HIV-1mt ZA012-P19 are
962 schematically represented (upper two diagrams). The region from the initiation of *vpr* to
963 the end of *env* that included recombination breakpoint sites is depicted in the third
964 diagram; the HIV-1mt ZA012-P0 (17 SGA sequences) or HIV-1mt ZA012-P19 (seven

965 SGA sequences) are depicted (bottom). Sequences from HIV-1mt ZA012-P0 were
966 classified into seven patterns of recombination breakpoints (R1 to R7). Sequences from
967 HIV-1mt ZA012-P19 were classified into one recombination breakpoint pattern (R8).
968 The numbers (left) indicate the numbers of sequences per analyzed sequence.
969
970 **Fig 5. Phylogenic analysis of partial *env* sequences.** A neighbor-joining phylogenic
971 tree was constructed from the partial nucleic acid sequences of *env* (nucleotide positions
972 211–2571 based on *env* of HXB2 numbering). The sequences of HIV-1 97ZA012
973 (white circle), HIV-1mt ZA012-P0 (grey circle) and HIV-1mt ZA012-P19 (black circle)
974 were determined from SGA sequences. HIV-1 97ZA012 (accession number:
975 AF286227) and 98CN007 (AF286230) reference sequences were obtained from the Los
976 Alamos HIV sequence database (http://hiv-web.lanl.gov/). R1–R8 correspond to the
977 patterns of recombination breakpoint types in Figure 2. Bootstrap values were computed
978 from 1,000 bootstrap replicates, and only > 90% are shown at branches. The scale bar
979 indicates the substitutions per site.
980

981 **Fig 6. Co-receptor usage of HIV-1mt ZA012-P19.** Infectivity of HIV-1 NL4-3,

982 SIVmac239 and HIV-1mt ZA012-P19 to TZM-bl cells was assessed in the presence of

983 increasing amounts of AMD3100 (CXCR4 inhibitor), AD101 (CCR5 inhibitor) or both.

984 The experiment was conducted in triplicate.

985

986 **Fig 7. HIV-1mt ZA012 infection of pig-tailed macaques.** Two pig-tailed macaques

987 were inoculated intravenously with HIV-1mt ZA012 (100,000 $TCID_{50}$), and the plasma

988 viral RNA burdens (A) and circulating $CD4^+$ T-lymphocytes (B) were monitored.

Figure1
Click here to download Figure: Figure1.pdf

Figure 1

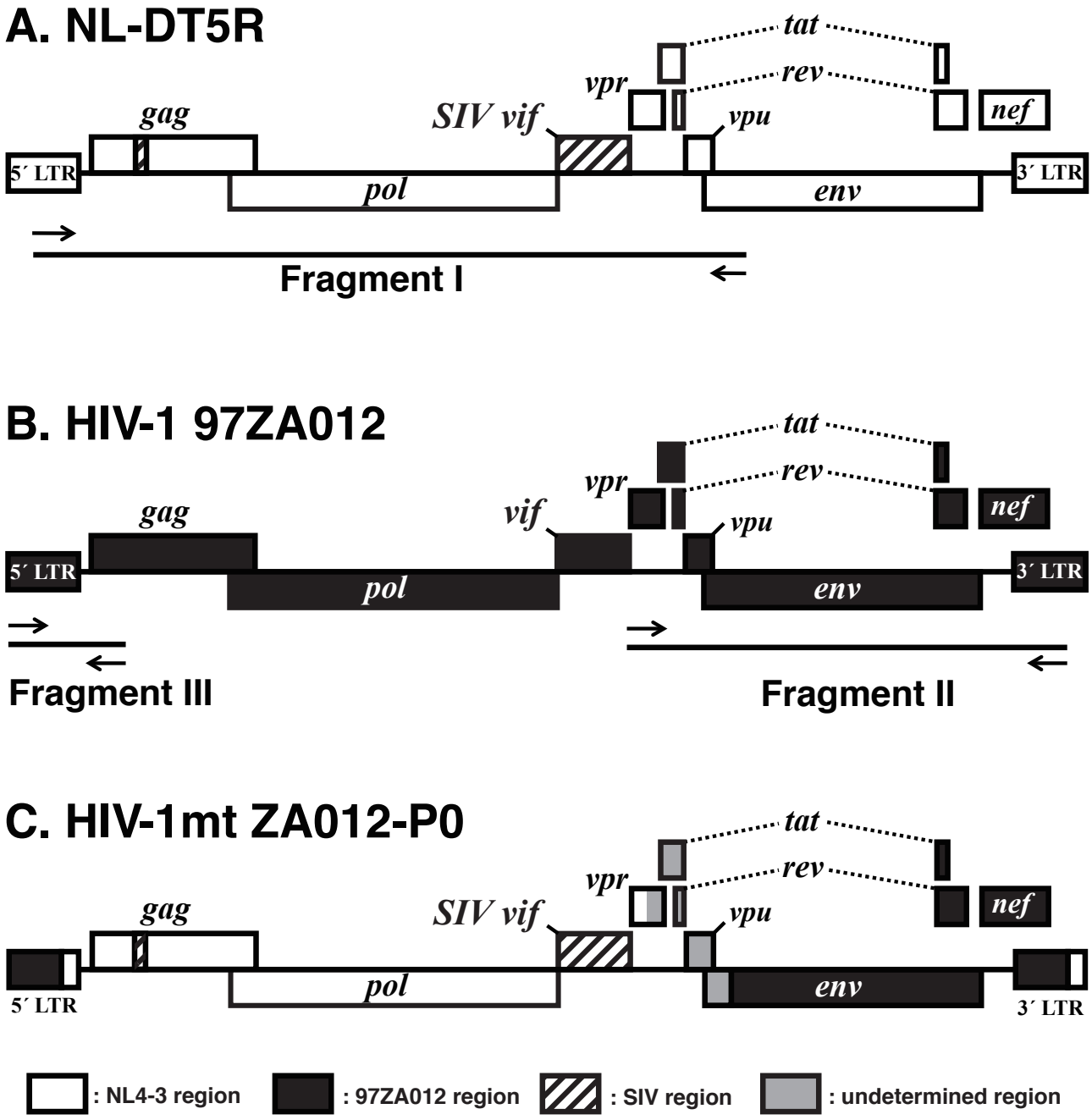

Figure2
Click here to download Figure: Figure2.pdf

Figure 2

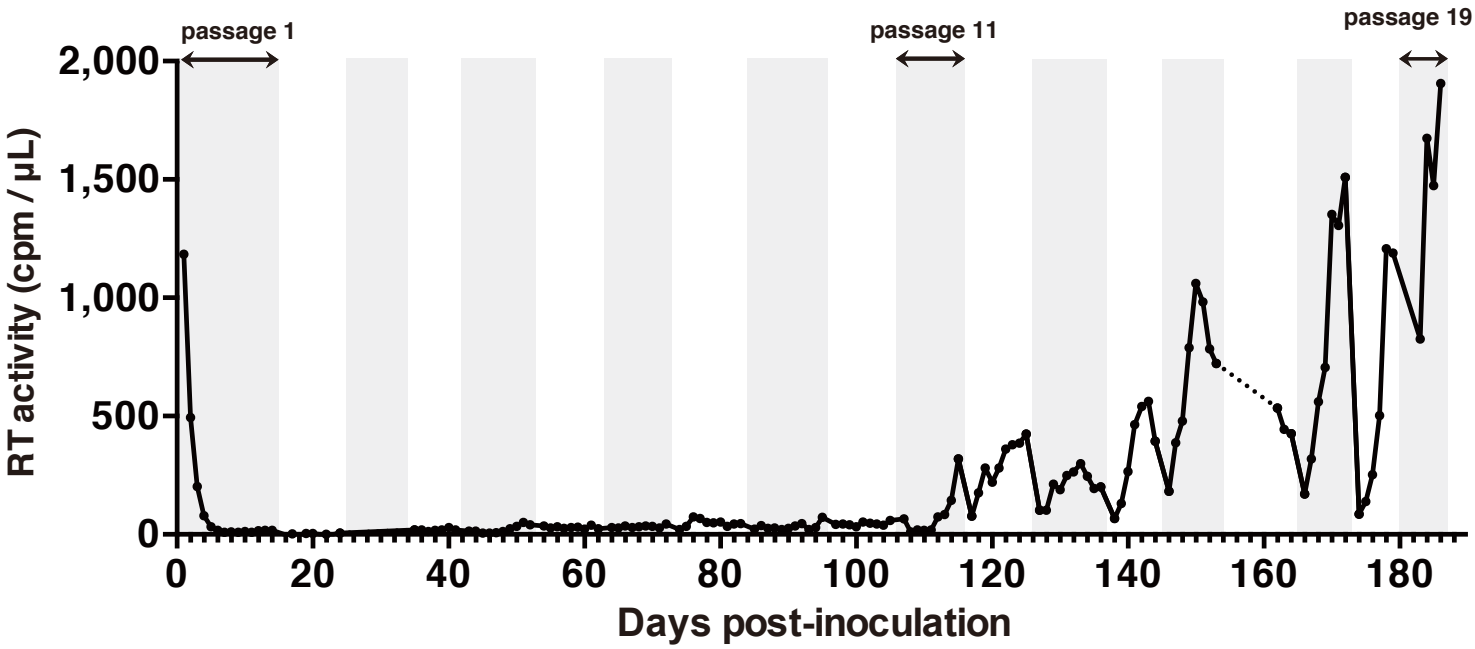

Figure3
Click here to download Figure: Figure3.pdf

Figure 3

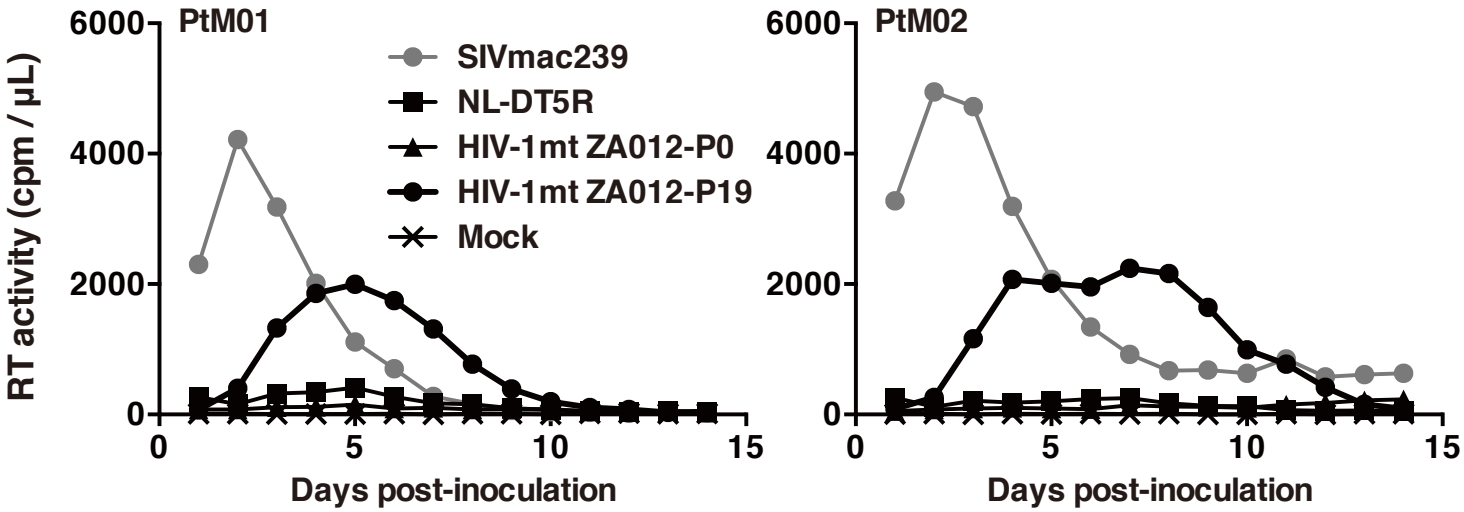

Figure4
Click here to download Figure: Figure4.pdf

Figure 4

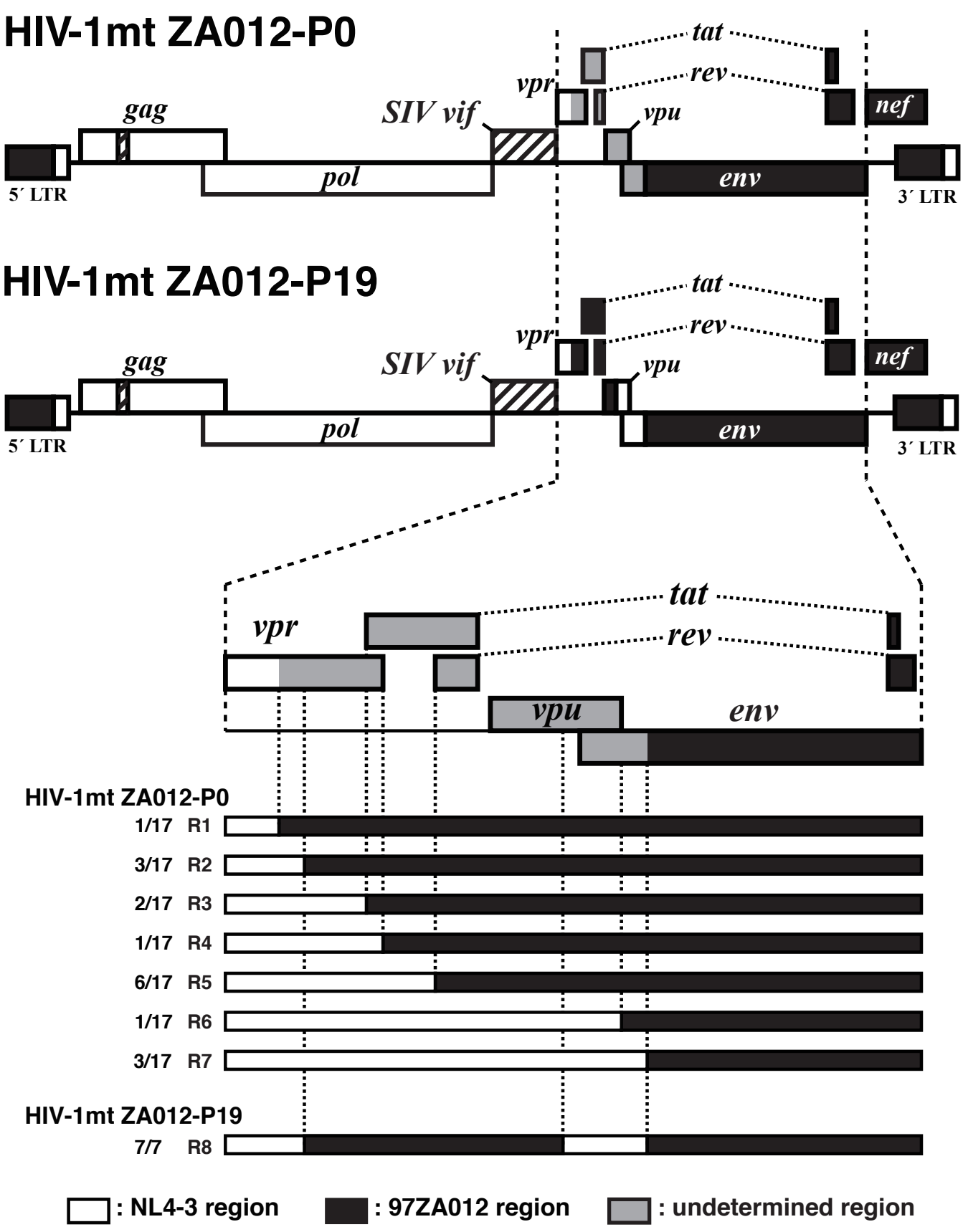

Figure5
Click here to download Figure: Figure5.pdf

Figure 5

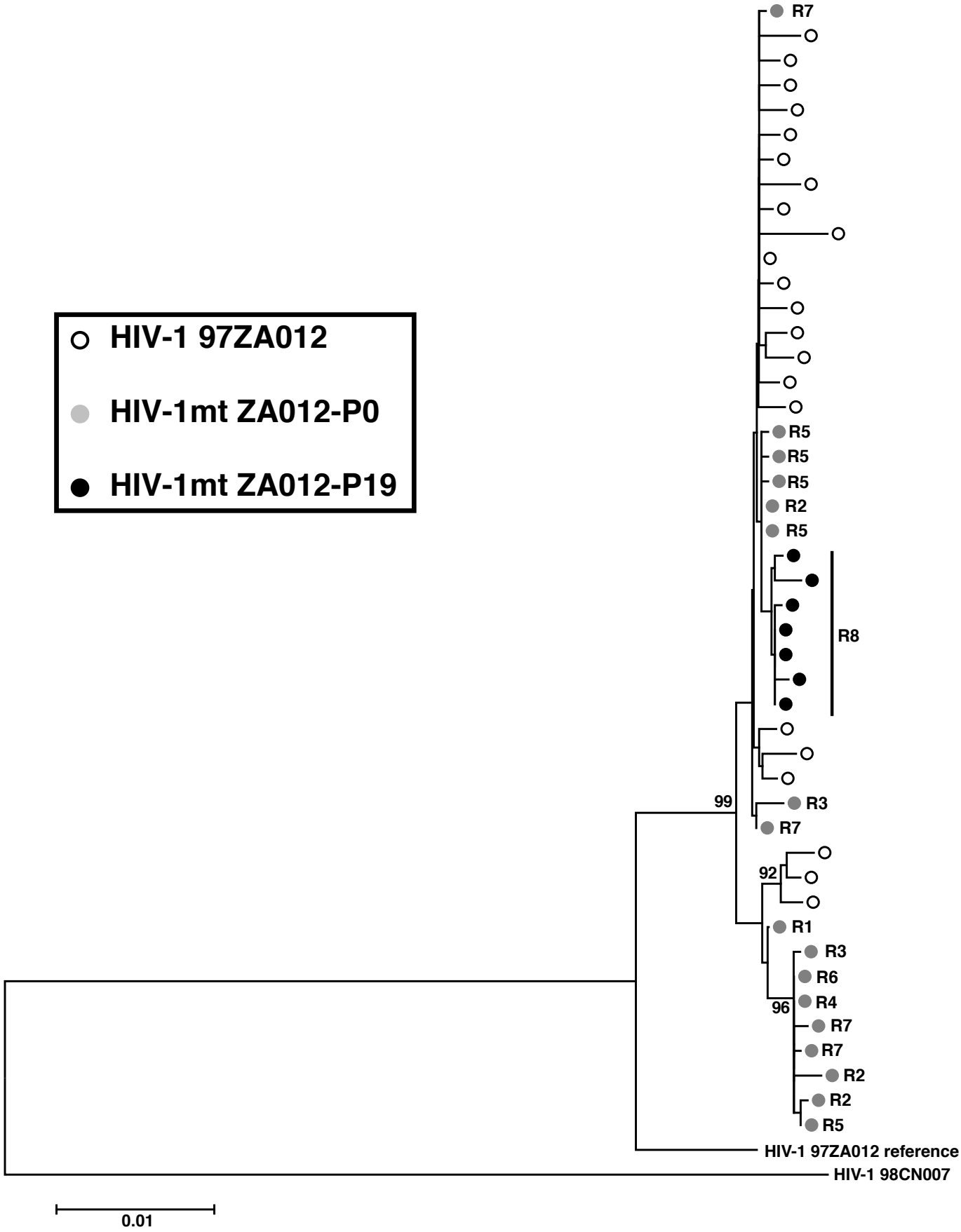

Figure6
Click here to download Figure: Figure6.pdf

Figure 6

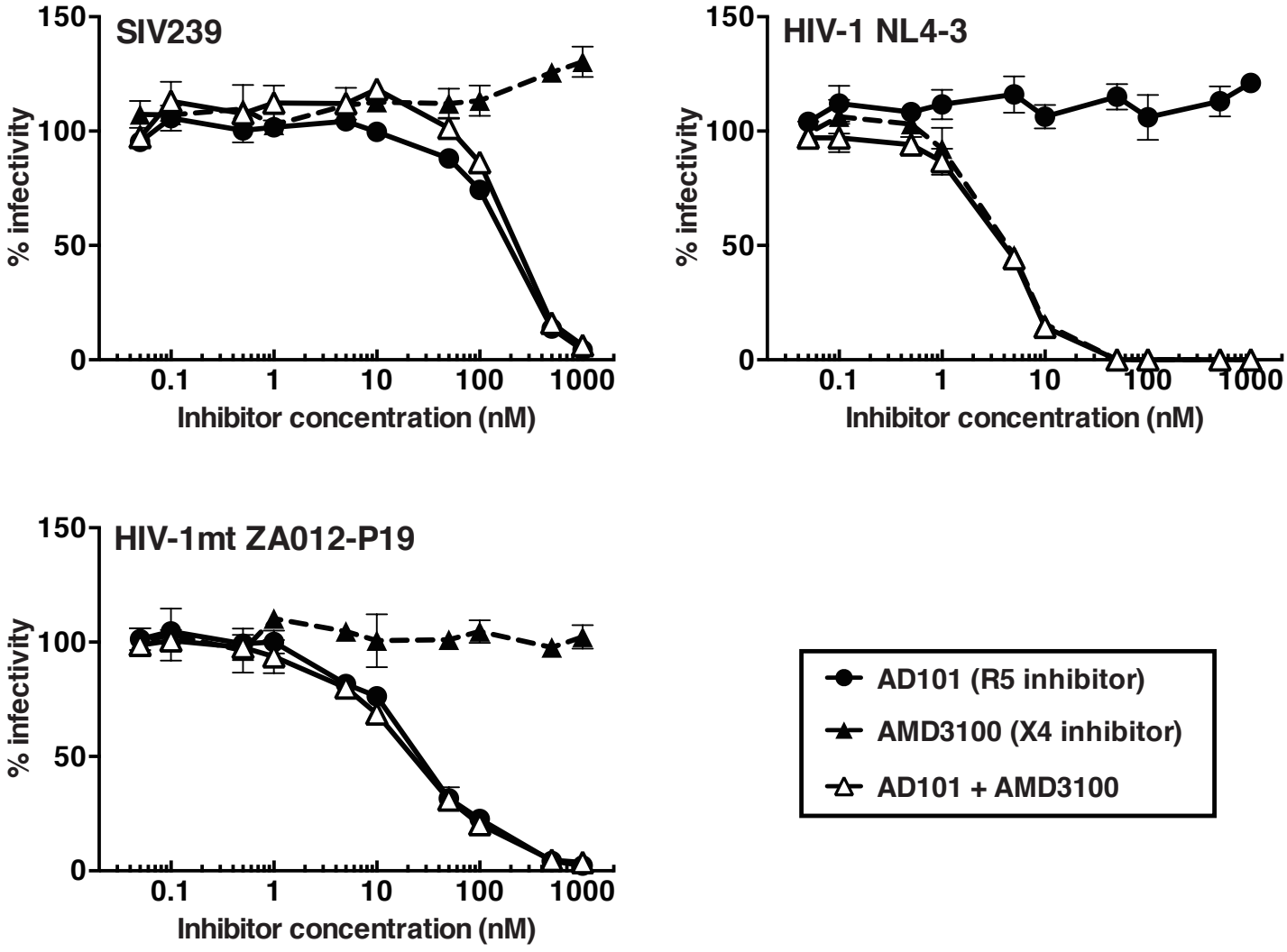

Figure7
Click here to download Figure: Figure7.pdf

Figure 7